Available online at www.sciencedirect.com

ScienceDirect

Energy Procedia 101 (2016) 1079 – 1086

Energy Procedia

71st Conference of the Italian Thermal Machines Engineering Association, ATI2016, 14-16 September 2016, Turin, Italy

A PCM thermal storage for ground-source heat pumps: simulating the system performance via CFD approach.

Emanuele Bonamente[a,*], Andrea Aquino[a], Franco Cotana[a]

[a]*CIRIAF – Engineering Department, University of Perugia, Perugia 06135 Italy*

Abstract

The conventional design of ground source heat pumps (GSHPs) is based on the peak heating and cooling loads. A possible optimization in GSHP design, including a thermal storage device between the ground exchangers and the heat pump, was already realized and it was found that a reduced-size geothermal field (-66%) is still able to cover the energy demand. In this paper, the design of the prototype was used as a starting point to study the potentialities of two possible upgrades for the optimization of the energy performance (COP) of the system. In the first case, the thermal storing material is water, as in the working prototype, and the efficiency is improved removing the cylindrical heat exchangers that were designed to separate the ground side from the heat pump side. In the second case, a completely new and more compact thermal storage was designed using phase change materials (PCMs). Computational fluid dynamics (CFD) simulations were performed in a transient regime to validate the model against observed data and to assess the potentiality of the two improvements. The system behavior is studied in terms of driving energy input and output energy production. Significant improvements of the system COP are observed (up to +20%). In the first case (water thermal storage), the overall COP is 4.1 during winter and 5.7 during summer, in the second case (PCM thermal storage), the COP is 4.1 and 5.9, respectively. The PCM thermal storage, in particular, is approximately 10 times smaller than the original design, and could be easily placed within the technical room.

Peer-review under responsibility of the Scientific Committee of ATI 2016.

Keywords: Ground source heat pumps (GSHP); Geothermal energy; Phase change materials (PCM); Computational fluid dynamics (CFD); Renewable energy sources; Thermal energy storage (TES); Air conditioning.

* Corresponding author. Tel.: +39-075-585-3576; fax: +39-075-585-3697.
E-mail address: emanuele.bonamente@unipg.it

Peer-review under responsibility of the Scientific Committee of ATI 2016.
doi:10.1016/j.egypro.2016.11.147

1. Introduction

The reduced emissions associated to renewable energy systems [1], such as the exploitation of geothermal energy [2], makes them the only viable alternative to fossil fuels [3]. As of 2012, the share of geothermal energy in the world total power production is still very low (0.3%), corresponding to 1.5% if considering renewable resources only [4]. However, the potential of geothermal energy goes well beyond this value [5]-[7], and a more diffuse exploitation could be easily obtained if some limitations, mainly due to high investment costs, could be overcome. The United States have the largest installed capacity of geothermal applications, corresponding to 28.8% of the worldwide share, and the second largest installed capacity for geothermal direct utilization (24.6%). China is the first country for direct geothermal utilization (25.2% of the total), with an installed capacity of 17,870 MW_{th} [4]. The exploitation of high- and medium-temperature geothermal resources is subject to their presence in site as they are not evenly distributed around the world. On the other hand, low-temperature geothermal resources are almost everywhere and are more easily exploitable as they are present in the very first layer of the earth crust. However, low-temperature geothermal resources are not directly exploitable, and they need a heat pump [8] to produce the required temperature levels. In this context, a common setup is given by ground source heat pumps (GSHPs). GSHPs use a ground heat exchanger to extract heat from the ground, a heat pump, and the distribution system. Two configuration are usually available for the ground heat exchangers: in case of exchange of both energy and matter with the ground, the system is defined as open-loop, requiring a production and a reinjection well; in case of exchange of energy only, the fluid circulates inside a closed-loop exchanger. Vertical closed-loop heat exchangers can also be referred to as boreholes.

GSHPs are able to efficiently exploit low-temperature geothermal energy in a large range of ground source temperatures (5 to 30°C) as it is, as a function of the latitude, almost everywhere in the world [9]. The efficiency of a heat pump is usually measured by the ratio of thermal energy available for heating or cooling use ($E_{th}^{building}$) and the heat pump driving energy consumption (E_{el}^{HP}):

$$COP = \frac{E_{th}^{building}}{E_{el}^{HP}} \tag{1}$$

where *COP* is the coefficient of performance. As a function of project parameters, such as latitude, soil properties, heat exchanger layout, and system size, the COP ranges from 3 to 6 for common applications [10]. At moderate latitudes, GSHPs show higher COPs during cooling cycles, because of the larger difference between air and ground temperature with respect to heating periods. The production of geothermal energy from GSHPs has shown an increasing trend (+17.6% per year in the US) in the period 2000-2009 [11].

The main limitation of the use of GSHPs is the installation cost. Borehole drilling alone can contribute up to 50% of the total investment cost [12]. An innovative approach for the design of GSHPs was already followed to implement a working prototype in service of a commercial building [13]. The conventional GSHP layout requires a sizing of the geothermal field (i.e. borehole depth) able to cover the maximum thermal power request during coldest or hottest periods of the year. In other words, the borehole depth and number must be sized such to produce enough power to cover load peaks. However, on average, thermal energy is exploited at a rate well below the maximum capacity, and the system daily duty cycle (e.g. E_{th}/E_{th}^{max}) is well below 100% even during coldest or hottest days. The proposed layout introduced a heat thermal storage to decouple the heat pump from the borehole field. While heat is continuously transferred to the storage by a reduced-size geothermal installation, the system is able to cover maximum power peaks. It is found that the borehole depth can be reduced up to 66%, still preserving the system energy performance. The first prototype used water as storage component. The presence of heat exchangers within the storage and the variation of water temperature during the operating cycle caused some limitations to the system operating performance. In this work, two alternative approaches are proposed to overcome these limitations and their potentialities are evaluated using a computational fluid dynamics approach.

2. The reference scenario

A working prototype of an innovative GSHP, designed to include a heat-storage device, was used as the starting point of this analysis. The prototype was realized within the *SCER* research project, and it has been successfully used

to satisfy heating and cooling requirements of the building for a 2-year time period [13],[14]. Unlike conventional GSHPs that are sized to cover thermal peaks, the innovative approach is based on the average daily load and a continuous exchange of heat with the ground. Ground heat exchangers are connected to a heat storage (a 12 m^3 underground tank filled with water) and the heat pump uses the stored heat upon request (Fig. 1). The geothermal system was specifically designed to respond two different requirements: the test, in real working conditions, of the performance of the innovative GSHP layout and the possibility to easily switch the system to the conventional layout in case of malfunctioning. For this reason, water circulating ground heat exchangers and heat pump was separated from the water in the tank using two cylindrical heat exchangers (Fig. 2). This double-loop configuration was realized to allow the bypass of the heat storage and revert the system to the conventional layout (heat pump directly connected to boreholes). For the same reason, a total of three 120-m boreholes were realized even if only 1 borehole is needed when the heat storage is used. The working logic of the system varies from heating (winter) to cooling (summer) mode. In winter, the heat pump takes the required heat from the storage. When the water temperature goes below the set temperature the borehole circulating pump is switched on and it is turned off when the set temperature is reached back. During part of the daily cycle, when the heating load is maximum, the geothermal power, generated from 1 borehole only, is lower than the power requested by the heat pump, and the tank temperature decreases. For the rest of the time, however, the borehole can continue to refill the heat storage, and initial conditions are reached at the end of the cycle. In cooling cycles, the system works in reverse mode.

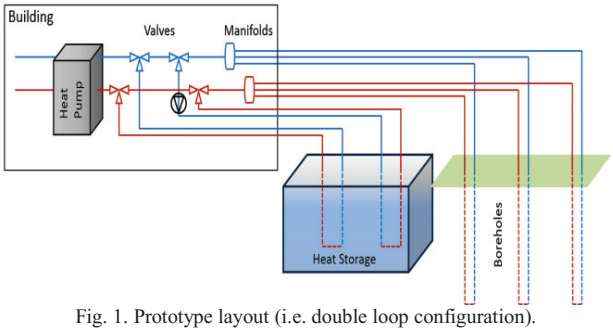

Fig. 1. Prototype layout (i.e. double loop configuration).

As an example of the system performance measured in the period 2013-2015, the summer COP_{tot}, including all the auxiliary apparatuses was 3.87 (May-September 2013), and the winter COP_{tot} was 3.81 (October-December 2013). The total system COP (equation 2) was found to be less than conventional applications. Even if the system was proved to be stable from an energy-balance point of view (the initial conditions are reached at the end of the cycle), the high electric energy consumption deteriorates the COP and makes the system not economically competitive. Two possible upgrades of the present layout are proposed in this paper, and the performances are evaluated using CFD simulations.

$$COP_{tot} = \frac{E_{th}^{building}}{E_{el}^{HP} + E_{el}^{BH}} \tag{2}$$

3. System upgrades and performance assessment

Two upgrades of the reference layout are proposed to overcome the limitations encountered during the monitoring period of the prototype. With respect to the original design (double-loop layout), the first upgrade consists in the removal of the cylindrical heat exchangers from the tank, resulting in a single-loop layout in which the same water circulates inside the heat pump, the heat storage, and the boreholes. A second upgrade is also considered using phase change materials (PCM [15],[16]) instead of water as active thermal storage (PCM layout).

A computational fluid dynamics approach was used to estimate the system performance of the heat storage for the three layouts. The Ansys Fluent version 16.0 software was used to run the simulations. The methodology is split into four phases: (i) the CFD model is first validated against observed data for heating and cooling cycles; (ii) the performance of the single-loop layout is simulated using the same boundary conditions as in the previous case; (iii)

typical operating conditions are used to analyze the single-loop system behavior in standard applications; (iv) the PCM layout is simulated for the same working conditions.

The double-loop geometry (Fig. 2a) was implemented considering the same design of the prototype [13],[14]. The heat storage is a quasi-cubic cement tank with 0.12 m walls and a carriageable 0.2 m roof. The inner capacity is 12.5 m^3. The system shows, with good approximation, an adiabatic behavior during both heating and cooling modes. Two inner heat exchangers are connected to the heat pump, on one side, and to the boreholes, to the other side. The contact surface of each exchanger is 20.15 m^2.

The single-loop geometry is the first improvement of the original layout, and it was realized removing of the heat exchangers (Fig 2b). The main reason for the low COP of the prototype is the temperature shift between the tank water temperature and the water circulating the two loops (i.e. heat pump and boreholes). In this layout, the tank water is directly sent to the heat pump and to the boreholes with no temperature shift. A cubic cement tank was modeled considering a constant wall thickness (0.12 m) and a total capacity of approximately 12.2 m^3.

The PCM layout represents the final improvement of the system (Fig. 2c). The completely new design of the heat storage reduces the storage volume (and the related excavation costs and land use) and furtherly improves the system COP. Phase change materials are characterized by a large range of possible transition temperatures (solid/liquid), particularly favourable for this kind of application. The twofold benefit is represented by the very reduced volume needed for the thermal storage and temperature-stabilization properties. In the transition region, PCMs can exchange energy in form of latent heat (in general >100 kJ/kg/K [17],[18]) instead of sensible heat, resulting in more than 10 times the energy needed to heat or cool the same mass of liquid water by the same temperature. At the same time, an appropriate choice of the PCM would guarantee that the temperature of the storage remains more stable during the entire working cycle, increasing the COP. The sizing of the PCM heat storage was performed considering typical working conditions: 80 kWh/day in heating mode and 50 kWh/day in cooling mode. Two stack of PCMs with different transition temperatures are used for the storage. The first (PCM_{heat}) melts at 8.25°C, the second (PCM_{cool}) melts at 25.25°C. Commercially-available Rubitherm^{TM} paraffins [19] were used to model the thermal properties of the two PCM stacks considering a transition range of 0.5°C. Minimum PCM volumes to support the heating and cooling cycles are 0.39 and 0.29 m^3, respectively.

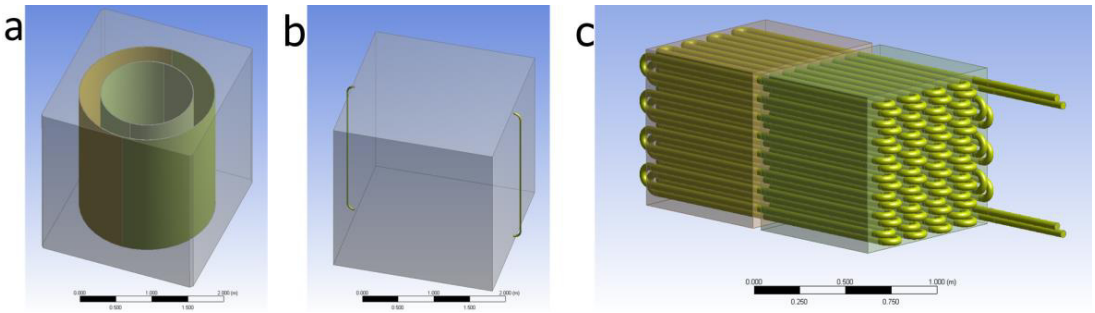

Fig. 2. (a) double-loop layout geometry; (b) single-loop geometry; (c) PCM layout geometry.

4. Results

4.1. Model validation

The validation of the CFD model was performed via the comparison of simulation results of the double-loop configuration and measured data. The same operating conditions observed from a 29-hour heating cycle (January 1st, 2014 3:00am to January 2nd, 2014 8:00 am) and a 45-hour cooling cycle (August 31st, 2014 3:00 am to September 2nd, 2014 0:00 am) were used to perform transient-regime simulations using a 300s time step. Results for the heating cycle are shown in Fig. 3a. The cooling cycle is shown in Fig. 4. Detailed results are shown in Table 1.

The first part of this analysis consists in the simulation of the single-loop layout using same boundary conditions as in section 4.1. The borehole performance was modeled as a function of inlet water temperature as recorded by the monitoring system during the period (Fig. 4). A linear interpolation of data was performed. For the heating mode,

since observed data do not cover the simulated temperature range, an extrapolation to lower temperatures was performed considering a zero thermal yield at the undisturbed ground temperature (15.5°C).

Table 1. Validation of the double-loop model: comparison with measured data.

		Heating mode		Cooling mode	
Start time		20/1/14 3:00		31/8/14 2:36	
End time		21/1/14 8:00		1/9/14 23:59	
Indoor thermal energy	(kWh)	130.78		-62.20	
Heat pump thermal energy	(kWh)	-92.08		72.38	
Heat pump electric energy	(kWh)	38.71		10.17	
Heat pump COP		3.38		6.11	
Borehole thermal energy	(kWh)	81.15		9.36	
Borehole electric energy	(kWh)	6.97		9.36	
Borehole duty cycle		0.91		0.78	
System COP		2.86		3.18	
		Heating mode		**Cooling mode**	
		data	sim	data	sim
Start temperature	(°C)	7.80	7.80	24.00	24.00
End temperature	(°C)	7.25	7.20	23.20	23.29
Min temperature	(°C)	6.20	6.31	21.90	21.90

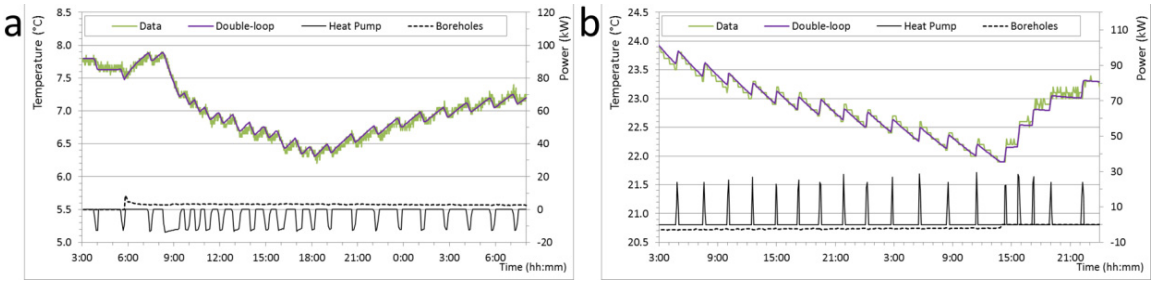

Fig. 3. (a) Heating-mode validation and (b) cooling-mode validation: measured (green) and simulated (purple) water temperature.

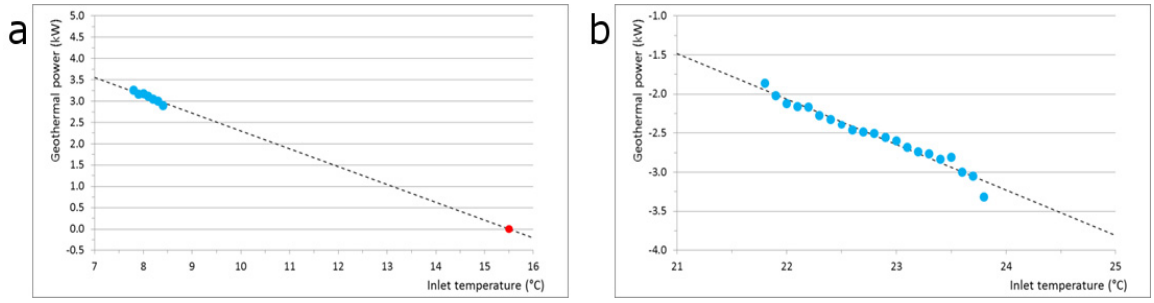

Fig. 4. Borehole yield vs inlet water temperature for the heating (a) and cooling (b) modes.

The comparison between heating mode results for double- and single-loop layouts, obtained using real boundary conditions, is shown in Fig. 5a. Except for the initial period, the temperature of the water in the single-loop storage tank is constantly higher than the double-loop configuration, while the two systems are providing exactly the same energy to the building. This difference depends on the average difference in the borehole inlet temperature, which is lower for the single-loop configuration (7.1°C with respect to 8.4°C of the double-loop case). According to Fig. 4a, this difference allows a higher power to be extracted from the ground. The system COP, thanks to the higher temperature of the water sent to the heat pump (4.5°C vs 7.2°C of the double-loop case), increases from 2.9 to 3.4.

A comparison of the cooling-mode results is shown in Fig. 5b. In this case, the water temperature of the single-loop case decreases more rapidly than the double-loop case. The average borehole inlet temperature in the first part of the cycle is lower than the double-loop case, producing a higher power dissipation in the ground, as shown in Fig. 4b (*right*). As a result, the set temperature (21.9°C) is reached approximately 3 hours earlier, the average heat pump

inlet temperature decreases from 24.0 to 22.7°C, and the resulting COP increases from 3.18 to 3.41. A summary of results is shown in Table 2. Typical schedules for heating and cooling modes were simulated using the Energy Plus software package after a recognition of the building characteristics [20]. Average daily heating and cooling loads during the most severe periods of the year are 80 kWh/day and 50 kWh/day, respectively. The typical thermal yield of boreholes was also estimated using a larger dataset, considering only those periods when the system was operated with the heat storage included. Results are shown in Fig. 6. A comparison between the results of single-loop and PCM configuration using typical boundary conditions is presented in next section.

Table 2. Real case: double-loop vs single-loop layout.

		Heating mode		Cooling mode	
		double-loop	single-loop	double-loop	single-loop
Indoor thermal energy	(kWh)	130.78	120.82	-62.20	-62.55
Heat pump thermal energy	(kWh)	-92.08	-92.08	72.38	72.38
Heat pump electric energy	(kWh)	38.71	28.74	10.17	9.82
Average inlet temperature	(°C)	4.54	7.18	23.99	22.77
Heat pump COP		3.38	4.20	6.11	6.37
Borehole thermal energy	(kWh)	81.15	91.75	-85.89	-81.10
Borehole electric energy	(kWh)	6.97	6.95	9.36	8.52
Borehole performance	(kWh_{th}/kWh_{el})	11.64	13.20	9.18	9.52
Average inlet temperature	(°C)	8.36	7.14	22.77	22.78
Borehole duty cycle		0.91	0.91	0.78	0.71
System COP		2.86	3.39	3.18	3.41

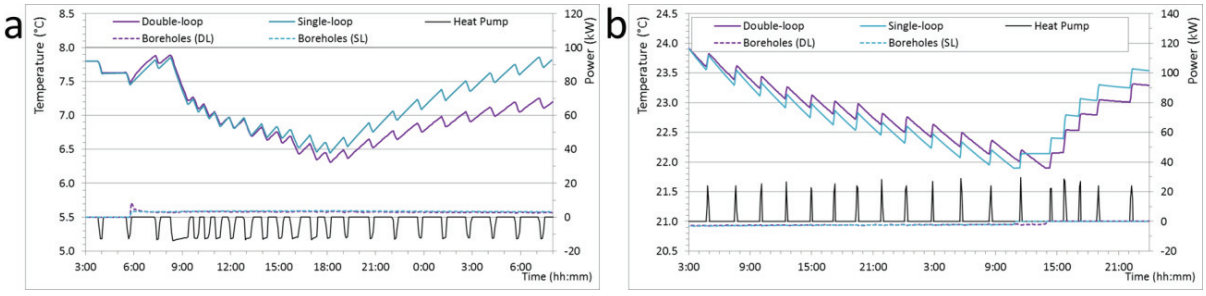

Fig. 5. (a) Heating and (b) cooling mode (real-case): double-loop (purple) and single-loop (blue) comparison.

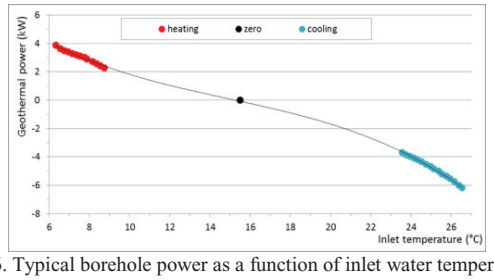

Fig. 6. Typical borehole power as a function of inlet water temperature.

4.2. PCM simulations

In the PCM layout, water circulates, in counter-flow mode, inside two serpentines that are surrounded by two stacks of phase change materials. The volume of each PCM stack is approx. 0.5 m^3. In the simulation, a difference between outlet and inlet temperatures of each serpentine reproduces the energy exchanged with the heat pump and with the boreholes. In heating mode, the borehole is turned on when the heat pump inlet temperature is below T_{ON}=8.4°C, and it is turned off when it is above T_{OFF}=8.5°C. In cooling mode, the logic is reversed: T_{ON}=25.1°C and T_{OFF}=25.0°C. The time step is 60s. The power exchanged with the ground, as a function of borehole inlet temperature, is modelled according to Fig. 6. PCMs were modelled as solid materials for which an empirical sensible heat curve was modelled to take into account the latent heat associated to melting/solidification (approx. 300

kJ/m^3/K within a 0.5°C region) according to data reported in Table 3. The transition of the PCM materials is reproduced by this modified sensible heat curve within the transition region (±0.25°C with respect to the reference transition temperature). The fraction of PCM in liquid phase (β) for $T_{solid}<T_{PCM}<T_{liquid}$ is given by

$$\beta = \frac{T_{PCM} - T_{solid}}{T_{liquid} - T_{solid}} \tag{3}$$

With respect to the real case simulation, an alternative and more efficient circulating pump [21] is used for the borehole circuit. A comparison of heating-cycle results with the single-loop geometry is shown in Fig. 7a. The total COP is 4.13, the liquid fraction of PCM_{heat} at the start of the cycle is 0.7 and it reaches a minimum of 0.1. The cooling mode is shown in Fig. 7b. The total COP is 5.89, the liquid fraction of PCM_{cool} at the beginning of the cycle is 0.2, with a maximum of 0.7. Detailed results are given in Table 4.

Table 3. Thermal properties of phase change materials used for the PCM layout.

Name	Material	Melting range (°C)	Heat of fusion (kJ/kg)	Sensible heat (kJ/kg)		Density (kg/m^3)	
				solid	liquid	solid	liquid
PCM_{heat}	RT6	8.0–8.5	140	1.8	2.4	860 @ -15°C	770 @ 15°C
PCM_{cool}	RT27	25.0–25.5	146	1.8	2.4	870 @ 15°C	750 @ 70°C

Table 4. Real case: single-loop vs PCM layout.

		Heating mode		Cooling mode	
		single-loop	PCM	single-loop	PCM
Indoor thermal energy	(kWh)	80.00	80.00	-50.00	-50.00
Heat pump thermal energy	(kWh)	-60.85	-60.88	58.04	58.01
Heat pump electric energy	(kWh)	18.68	18.65	8.33	8.31
Average inlet temperature	(°C)	8.09	8.18	25.27	25.17
Heat pump COP		4.28	4.29	6.00	6.02
Borehole thermal energy	(kWh)	60.27	61.37	-57.30	-59.57
Borehole electric energy	(kWh)	0.75	0.74	0.39	0.39
Borehole performance	(kWh_{th}/kWh_{el})	80.36	82.93	146.92	152.74
Average inlet temperature	(°C)	7.98	7.83	25.42	25.68
Borehole duty cycle		0.89	0.88	0.47	0.47
System COP		4.12	4.13	5.73	5.89
Start PCM liquid fraction		*n.a.*	0.669	*n.a.*	0.188
Stop PCM liquid fraction		*n.a.*	0.647	*n.a.*	0.189
Minimum PCM liquid fraction		*n.a.*	0.094	*n.a.*	0.129
Maximum PCM liquid fraction		*n.a.*	0.671	*n.a.*	0.667

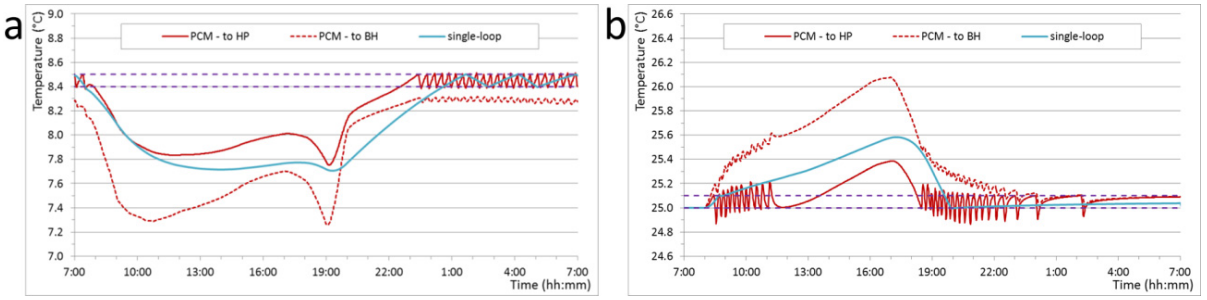

Fig. 7. (a) heating and (b) cooling cycle: PCM (red) and single-loop (blue) water temperature simulated using the ideal-case schedule.

5. Discussion and conclusions

The dynamic operation of an innovative layout for GSHPs, including a heat storage device, was simulated using a CFD approach in transient regime. A prototype of the system was already implemented and monitored and it is currently used for a commercial building. Two possible upgrades of the system, designed to overcome some limitations to the global performance (COP) are proposed and simulated.

The CFD model of the prototype was first validated against measured data. Results show a good agreement between simulations and observations. The first upgrade of the heat storage consists in the removal of the heat exchangers, required in the original design for safety reasons. In this configuration, the thermal shift between the water in the tank and the water in borehole and heat pump circuits is removed. As a result, the heating mode simulation shows a significant increase of the borehole inlet temperature (+2.6°C) and the COP of the heat pump increases from 3.4 to 4.2. The resulting energy saving is approximately 20%. Similarly, the thermal exchange with the ground is more efficient (11.6 to 13.2 kWh_{th}/kWh_{el}), producing a 12% energy saving. The total system COP increases from 2.9 to 3.4. In cooling mode, the energy saving for the heat pump and the borehole pump is 4%. The system COP increases from 3.2 to 3.4. The same layout was also used to simulate heating and cooling cycles under typical working conditions and using a more efficient circulating pump for the boreholes. In this case the system COP is 4.12 and 5.73, respectively. A further improvement of the system was designed using a PCM heat storage. Two stacks of PCMs are used, with transition temperatures chosen to maximize the system performance in heating and cooling mode. Results, using typical working schedules, are consistent with the upgraded layout. Inlet temperatures are more stable and a slight increase of the system performance in achieved. The COP is 4.13 in heating mode and 5.89 in cooling mode. The total volume of the PCM heat storage is 10 times smaller than the water tank, and it could be easily placed indoor.

References

[1] Bonamente, E.; Pelliccia. L.; Merico, M.C.; Rinaldi, S.; Petrozzi, A. The Multifunctional Environmental Energy Tower: Carbon Footprint and Land Use Analysis of an Integrated Renewable Energy Plant. *Sustainability* **2015**, 7, 13564-13584.

[2] Wu, R. Energy efficiency technologies - air source heat pump vs ground source heat pump. *Journal of Sustainable Development* **2009**, 2, 14-23.

[3] Office of Energy Efficiency and Renewable Energy. Geothermal today. 2003 geothermal technologies program highlights. US Department of Energy, 2004, Washington.

[4] Jialing, Z.; Kaiyong, H.; Xinli, L.; Xiaoxue, H.; Ketao, L.; Xiujie, W. A review of geothermal energy resources, development, and applications in China: Current status and prospects. *Energy* **2015**, 93, 466-483.

[5] Muffler, P.; Cataldi. Methods for regional assessment of geothermal resources. *Geothermics* **1978**, 7, 53-89

[6] Hochestein, M.P. Classification ad assessment of geothermal resources. Small geothermal resources: A guide to development and utilization, UNITAR, 1990, New York

[7] Benderitter, Y.; Cormy, G. Possible approach to geothermal research and relative costs. Small Geothermal Resources: A Guide to Development and Utilization, UNITAR, 1990, New York.

[8] Stuart, J.S.; Bale, V.R.; Marc, A.R. Geothermal heat pump sytems: Status review and comparison with other heating options. *Applied Energy* **2013**, 101, 341-348.

[9] Hepbasli, A.; Kalinci, Y. A review of heat pump water heating systems. *Renewable Sustainable Energy Review* **2009**, 13, 1211-1229.

[10] Office of Energy Efficiency. Heating and cooling with a heat pump – ground source heat pumps (earth-energy systems). Ottawa, CA: Natural Resources Canada, 2009.

[11] U.S. Energy Information Administration. Geothermal Heat Pump Manufacturing Activities 2009.

[12] Bu, X.; Ma, W.; Li, H. Geothermal Energy production utilizing abandoned oil and gas wells. *Renewable Energy*, **2012**, 41, 80-85.

[13] Moretti, M.; Bonamente, E.; Buratti, C.; Cotana, C. Development of innovative heating and cooling systems using renewable Energy sources for non-residential buildings. *Energies* **2013**, 6, 5114-5129.

[14] Bonamente, E.; Moretti, E.; Buratti, C.; Cotana, F. Design and Monitoring of an innovative geothermal system including an underground heat-storage tank. *International Journal of Green Energy* **2016**, 13(8), 822-830.

[15] Cabeza, L.F.; Castell, A.; Barreneche, C.; De Gracia, A.; Fernandez, A.I. Materials used as PCM in thermal Energy storage in buildings: a review. *Renewable Sustainable Energy Reviews* **2011**, 15, 1675-1695.

[16] Murat, K.; Khamid, M. Passive thermal control in residential buildings using phase change materials. *Renewable and sustainable energy reviews* **2016**, 55, 371-398.

[17] Lee, T.; Hawes, D.W.; Banu, D. Feldman, D. Control aspects of latent heat storage and recovery in concrete. *Solar Energy Materials and Solar Cells* **2000**, 62, 217–237.

[18] Velraj, R.; Seeniraj, R.V.; Hafner, B.; Faber, C.; Schwarzer, K. Experimental analysis and numerical modeling of inward solidification on a finned vertical tube for a latent heat storage unit. *Solar Energy* **1997**, 60, 281–290.

[19] Kenisarin, M.; Mahkamov, K. Solar energy storage using phase change materials. *Renewable and Sustainable Energy Reviews* **2007**, 11, 1913–1965.

[20] Aquino, A. "Modellazione di un impianto geotermico sperimentale con accumulo di calore a servizio di un edifcio artigianale", MS thesis, Perugia University – Italy, 2013

[21] Grundfos UPS 20-60 N 150 – 96913096. Available online http://product-selection.grundfos.com/product-detail.html?productnumber=96913096&qcid=72649874